frontiers in Marine Science

ORIGINAL RESEARCH
published: 13 August 2018
doi: 10.3389/fmars.2018.00281

Phytoplankton σ_{PSII} and Excitation Dissipation; Implications for Estimates of Primary Productivity

*Kui Xu[1], Johann Lavaud[2], Rupert Perkins[3], Emily Austen[1], Marlène Bonnanfant[1,4] and Douglas A. Campbell[1]**

[1] Department of Biology, Mount Allison University, Sackville, NB, Canada, [2] UMI 3376 Takuvik CNRS, Université Laval, Département de Biologie, Québec, QC, Canada, [3] School of Earth and Ocean Sciences, Cardiff University, Cardiff, United Kingdom, [4] Mer-Molécules-Santé, Université de Maine, Nantes, France

The effective absorption cross section for photochemistry of Photosystem II in the light (σ_{PSII}') comprises the probability of light capture by Photosystem II and the quantum yield for subsequent photochemistry. σ_{PSII}' is used to model photosynthesis and aquatic productivity, and phytoplankters regulate σ_{PSII}' to mitigate over- or under-excitation of Photosystem II. We used diverse phytoplankton taxa to compare short and long term changes in σ_{PSII}' with the induction of the yield of non-photochemical quenching (YNPQ) of chlorophyll fluorescence, a measure of regulated excitation dissipation. In two picocyanobacteria σ_{PSII}' showed no decline upon induction of moderate YNPQ, above light levels sufficient for saturation of electron transport. In the eukaryotic chl a/b *Ostreococcus* and the chl a/c diatom *Thalassiosira,* induction of non-photochemical quenching was stronger after growth under saturating light, an acclimation attributable to increased xanthophyll cycle pigment content. Across short and longer-term light histories to induce or relax regulatory processes *Ostreococcus* and *Thalassiosira* showed proportional variations between the level of YNPQ and the down regulation of σ_{PSII}'. The proportional down regulation of σ_{PSII}' was, however, significantly smaller than the amplitude of YNPQ induction. For the eukaryotes we can predict changes in σ_{PSII}', useful for modeling electron transport, productivity and acclimation, from measures of YNPQ, which are accessible from fluorescence yield measures that do not include σ_{PSII}'. This useful relation, however, does not extend to the tested prokaryotes, possibly as a result of differential violations of the rate constant assumptions that underlie the calculated YNPQ parameter.

Keywords: chlorophyll fluorescence, diatoms, light acclimation, photosynthesis, picocyanobacteria, prasinophytes, *Prochlorococcus*

OPEN ACCESS

Edited by:
George S. Bullerjahn, Bowling Green State University, United States

Reviewed by:
Robert L. Burnap, Oklahoma State University, United States
Assaf Sukenik, Israel Oceanographic and Limnological Research, Israel

***Correspondence:**
Douglas A. Campbell
dcampbell@mta.ca

Specialty section:
This article was submitted to Aquatic Microbiology, a section of the journal Frontiers in Marine Science

Received: *31 May 2018*
Accepted: *23 July 2018*
Published: *13 August 2018*

Citation:
Xu K, Lavaud J, Perkins R, Austen E, Bonnanfant M and Campbell DA (2018) Phytoplankton σ_{PSII} and Excitation Dissipation; Implications for Estimates of Primary Productivity. Front. Mar. Sci. 5:281. doi: 10.3389/fmars.2018.00281

INTRODUCTION

The effective absorption cross section for Photosystem II (PSII) photochemistry is a target-size formulation which can be extracted from the chlorophyll fluorescence induction curve provoked by a single turnover flash or train of repeated flashlets (Kolber et al., 1998) applied in darkness (σ_{PSII}) or in the presence of actinic light (σ_{PSII}'). Because σ_{PSII} is estimated based upon the response of PSII to light it measures both the capture of light by the antenna bed associated with PSII, along with an implicit quantum yield for subsequent photochemistry (Trissl and Lavergne, 1995; Kolber et al., 1998; Laney, 2003; Suggett et al., 2009).

phytoplankton primary productivity and acclimation (Suggett et al., 2003, 2004, 2009; Oxborough et al., 2012; Silsbe et al., 2015). σ_{PSII} varies widely across species (Six et al., 2007a, 2008; Key et al., 2010) and changes through multiple short and longer term processes (Falkowski and Owens, 1980). In particular changes in growth light can cause compensatory changes in σ_{PSII}, as organisms allocate protein resources to light capture under limiting light, or to down-stream metabolism under saturating light (Falkowski and Owens, 1980).

Non-photochemical quenching (Horton et al., 1996; Gorbunov et al., 2011; Kirilovsky and Kerfeld, 2013) is a widely measured category of regulatory processes that are tracked through influences upon chlorophyll fluorescence (Miloslavina et al., 2009; Lambrev et al., 2012; Giovagnetti and Ruban, 2016). Non-photochemical quenching reflects changes in the dissipation of absorbed excitation as heat. There is a large literature across species and growth conditions (Ruban et al., 2004; Bailey et al., 2005; Lavaud et al., 2007; Kulk et al., 2012, 2013; Holzwarth et al., 2013; Lavaud and Lepetit, 2013; Giovagnetti and Ruban, 2016) reporting the patterns and responses of the unbounded Stern-Volmer parameterization, NPQ:

$$NPQ = (F_M - F'_M)/F'_M.$$

The NPQ parameter is not, however, a linear representation of the fraction of absorbed excitation flowing to non-photochemical quenching (Holzwarth et al., 2013). As an alternative, the fractional quantum yield of non-photochemical quenching (YNPQ, or Φ_{NPQ}) was introduced by Kramer et al. (2004) and re-formulated by Hendrickson et al. (2004) and Klughammer and Schreiber (2008). YNPQ is a bounded coefficient capturing excitation flowing to regulated non-photochemical dissipation of excitation through paths parameterized through the rate constant k_{npq}:

$$YNPQ = F_S/F'_M - F_S/F_M. \text{ (Hendrickson et al., 2004; Klughammer and Schreiber, 2008)}$$

The complementary yield of non-regulated excitation dissipation (YNO or Φ_{NO}) (Hendrickson et al., 2004; Klughammer and Schreiber, 2008) then captures non-regulated flows of excitation through thermal de-excitation paths parameterized through the rate constant k_d and through fluorescence, parameterized as k_f:

$$YNO = F_S/F_M.$$

Although termed non-regulated, YNO is not a constant, and can vary with changes in PSII photoinactivation, or with transitions from rapidly reversible quenching through k_{npq} to sustained non-photochemical quenching through k_d (Perkins et al., 2018). Finally, YPSII (or Φ_{PSII}) parameterizes the yield of excitation driving PSII photochemistry (Genty et al., 1989) through the k_p rate constant:

$$YPSII = (F'_M - F_S)/F'_M.$$

As coefficients that express the proportions of excitation flowing through three complementary paths, conservation of energy dictates that YNPQ + YNO + YPSII sum to 1, both algebraically and conceptually:

$$((F_S/F'_M) - (F_S/F_M)) + (F_S/F_M) + ((F'_M - F_S)/F'_M) = 1$$

Furthermore, algebraically, Stern-Volmer

$$NPQ = (F_M - F_M')/F_M' = YNPQ/YNO.$$

Thus the widely used Stern-Volmer NPQ actually captures the ratio between two sub-fractions of overall non-photochemical dissipation.

These calculated parameters reflect the combined influences of multiple mechanisms and kinetic phases (Boulay et al., 2008; Wu et al., 2012; Lavaud and Lepetit, 2013; Goss and Lepetit, 2015) whose relative influences vary with taxa and with physiological state. Differing growth lights can change the instantaneous capacity to induce non-photochemical quenching (Wu et al., 2012) through changes in the contents of key carotenoids and proteins that mediate non-photochemical quenching (Six et al., 2009; Wu et al., 2012; Kulk et al., 2013). Field studies are now using changes in measured non-photochemical quenching to help explain changes in the conversion of electron transport rates, based upon σ_{PSII}, to carbon-based marine productivity rate estimates (Schuback et al., 2015, 2016).

Explicit paired comparisons of Stern-Volmer NPQ with changes in σ_{PSII}' under illumination on the same samples (KoblížEk et al., 2001; Giovagnetti and Ruban, 2016) show that moderate induction of NPQ drives parallel down regulation of σ_{PSII}' but that levels of Stern-Volmer NPQ above ∼1 do not drive further down-regulation of σ_{PSII}'.

For this paper, we use the YNPQ yield parameterization because it is bounded from 0 to 1, and an increase in YNPQ in principle reflects a linear increase in regulated excitation dissipation. Nevertheless, in our experiments simultaneous determinations of YNPQ and Stern-Volmer NPQ were highly correlated (**Figure S1**) mainly because our treatments did not achieve the higher levels of measured Stern-Volmer NPQ (Ruban et al., 2004) where the departure from linearity would influence results.

An increase in YNPQ, or more generally an increase in (YNPQ + YNO) should cause a proportional decrease in σ_{PSII}', because σ_{PSII}' comprises both the absorption cross section of PSII, $a_{PSII,}$ and the maximum quantum yield for PSII photochemistry $YPSII_{max}$.

$$\sigma'_{PSII} = a_{PSII} \times YPSII_{max} = a_{PSII} \times F'_V/F'_M$$

Our paper aims to test this hypothesis, to determine whether changes in YNPQ can be used to model short-term changes in σ_{PSII}', to support productivity estimates under fluctuating conditions.

We also sought to systematically address several related questions:

1) Progressively increasing light drives an increase in excitation pressure ($1\text{-}q_L$) as delivery of excitation to PSII outruns

downstream electron transport. Does the threshold level of 1-q_L at which induction of YNPQ begins differ with taxa, and/or with growth light? Thereafter, does the slope of the induction of YNPQ vs. 1-q_L differ with species or with growth light, or both?

2) Does the relation between YNPQ and σ_{PSII}' differ systematically across taxa or with growth light?
3) During the relaxation of YNPQ in darkness following saturating light, does the decline in YNPQ correlate with a proportional increase in σ_{PSII}? Is this relationship symmetrical to that between YNPQ and σ_{PSII}' during induction, or is there a hysteresis between induction and relaxation? In other words, is there a consistent relation between instantaneous YNPQ and the degree of downregulation of σ_{PSII}', or does the light history path of the cells to reach a given level of YNPQ alter the relation? This last point is critical for modeling photophysiological responses of phytoplankton in dynamic environments such as coastal systems and the ocean upper layer.

MATERIALS AND METHODS

We grew four phylogenetically, structurally (Rast et al., 2015) and photophysiologically diverse marine phytoplankters (**Table 1**), using nutrient replete culture replicates previously described (Xu et al., 2017) in a temperature controlled incubator at 22°C. *Prochlorococcus* MED4 is a picocyanobacteria which captures light through Pcb divinyl chlorophyll a/b binding protein complexes (Ito and Tanaka, 2011) embedded within the thylakoid membranes. *Synechococcus* WH8102 is a picocyanobacteria which captures light through Phycobilisome (PBS) bilin-binding protein complexes associated with the surface of thylakoid membranes. *Ostreococcus* is a prasinophyte with a green primary endosymbiotic plastid, which captures light through chlorophyll a/b binding LHC proteins embedded within the thylakoids. *Thalassiosira pseudonana* CCMP1335 is a small centric diatom with a secondary endosymbiotic plastid derived from the red lineage. It captures light through chlorophyll a/c fucoxanthin binding proteins embedded within the thylakoids. These FCP complexes also mediate the large capacity for non-photochemical quenching typical of diatoms (Lavaud and Lepetit, 2013).

We applied a light/dark cycle of 12:12h, under either 30 μmol photons $m^{-2}s^{-1}$, representative of the bottom region of the photic zone, or under 260 μmol photons $m^{-2}s^{-1}$, equivalent to the middle of the photic zone. We chose these growth light levels as growth limiting or growth saturating light levels under our culture conditions, within the acclimatory tolerance ranges of the four diverse taxa (Six et al., 2009; Li and Campbell, 2013; Murphy et al., 2017). We tracked the growth of cultures by following fluorescence emission at 680 nm (*Prochlorococcus*, *Ostreococcus,* and *Thalassiosira*) or at 650 nm (*Synechococcus*) using a plate spectrofluorometer (SpectraMax Gemini EM, Molecular Devices, Sunnyvale, USA). Beyond these four taxa we include Supplementary Data from *Chorella vulgaris* (chlorophyte, chl a/b) (Bonnanfant and Campbell, unpublished); *Haslea ostrearia* and *Haslea* sp. (temperate and tropical pennate diatom strains, chl a/c) (Lavaud et al., unpublished) and *Micromonas* NCMA 2099 (arctic chl a/b Prasinophyte) (Ni et al., 2017). These strains were grown under comparable conditions, for different studies.

When cultures reached mid-exponential phase we took samples for whole cell absorbance measures in an integrating cavity spectrophotometer (OLIS-Cary14 with DSPC) (Ni et al., 2017). From these spectra we took second derivative spectra to detect changes in carotenoid absorbance resulting from xanthophyll cycling (Jesus et al., 2008). In parallel we took samples for chlorophyll fluorescence induction measurements, placed them in a 2 ml cuvette and then dark-adapted them for ∼2 min. Samples were then exposed to a train of 40 blue (455 nm) flashlets with a duration of 1.2 μs separated by an intervening interval of 1.0 μs of darkness to induce a Fast Repetition and Relaxation fluorescence (FRRf) induction curve (Kolber et al., 1998), using a Photon Systems Instruments FL3500 fluorometer system (Brno, Czech Republic). This train of 40 blue flashlets cumulatively induced a single turnover of PSII which reduced Q_A and thereby closed the PSII pool. We chose the intensity of the flashlet for each species in order to saturate the fluorescence rise within around 30 of 40 flashlets (**Figure 1**, insets) (Laney, 2003; Laney and Letelier, 2008). We chose 455 nm as a compromise excitation wavelength absorbed by the long side of the chlorophyll a (or divinyl chlorophyll a) absorbance band, which is the only pigment present across all our diverse study strains. Emerging multi-spectra chlorophyll fluorometers will support more generalized analyses across multiple excitation bands delivered through different antenna complexes (Simis et al., 2012) across taxa.

For each FRRf induction curve we exported the data from the FluorWin data capture software to fit a model with four parameters (**Table 2**): minimal fluorescence, F_0 (or F_S); maximal fluorescence, F_M (or (or F_M '); effective absorption cross section for PSII photochemistry, σ_{PSII} (or σ_{PSII}'); and the coefficient of excitonic connectivity ρ (Kolber et al., 1998) using the PSIWORX-R package (A. Barnett, sourceforge.net) (Murphy et al., 2016; Ni et al., 2017). For each measurement we did an FRRf induction before and then again after a 1 s period of darkness to allow PSII to re-open after illumination. We thus determined in the dark F_0, F_M, σ_{PSII}, ρ; under actinic light F_S, F_M', σ_{PSII}' ρ′; and following 1 s of darkness after actinic light F_0 ′1s, F_M ′1s, ρ′1s, σ_{PSII}′1s.

To account for possible rapid changes in non-photochemical quenching during the 1 s dark interruption we estimated F_0' as:

$$F_0' = F_{0\,1s}' * \{1 - [(F_{M\,1s}' - F_M')/F_{M\,1s}']\}$$

(Oxborough and Baker, 1997).

To examine the response of PSII function to increasing light intensity in the four studied species, we set a series of 60 s exposures to increasing steps of actinic light levels from 0 to a maximal light level (**Figure 1A**) again delivered at 455 nm to match the effective absorption cross sections measured using the FRR chlorophyll inductions. We measured the FRRf induction curve at the end of each light level exposure, and then again after

TABLE 1 | Key properties of Prochlorococcus, Synechococcus, Ostreococcus, and Thalassiosira.

Species	Diameter	Major pigments	Major antenna	State transition
Prochlorococcus MED 4	~0.6 μm	Chl *a*2, *b*2 (Morel et al., 1993)	Pcb	Not in MED4 (Rocap et al., 2003)
Synechococcus WH8102	~1 μm	Chl *a*, APC, PE (PEB and PUB) (Six et al., 2007b)	PBS	PBS movement, spillover (Li et al., 2004)
Ostreococcus RCC745	~1 μm	Chl *a*, *b* (Chrétiennot-Dinet et al., 1995)	LHCs	Not found (Swingley et al., 2010)
Thalassiosira pseudonana CCMP1335	~ 5 μm	Chl *a*, *c*	FCPs	Not found (Owens, 1986)

TABLE 2 | Table of abbreviations and parameters.

Parameter	Equation	Definition, units	References
a_{PSII}		Absorption cross section of PSII, A^2 photon^{-1} or A^2 PSII^{-1} (not to be confused with σ_{PSII})	Suggett et al., 2003
F_0		Minimal fluorescence with PSII open	van Kooten and Snel, 1990
F_M		Maximal fluorescence with PSII closed	van Kooten and Snel, 1990
F_S		Fluorescence at an excitation level	van Kooten and Snel, 1990
F_M'		Maximal fluorescence with PSII closed at an excitation level	van Kooten and Snel, 1990
$F_M'1s$		Maximal fluorescence with PSII closed 1 s after excitation	Murphy et al., 2016
$F_0'1s$		Minimal fluorescence with PSII open 1 s after excitation	Murphy et al., 2016
F_0'	$F_0/\{(F_M\text{-}F_0)/F_M + F_0/F_M'1s\}$	Minimal fluorescence with PSII open, estimated for cells under excitation, excluding cumulative influence of photoinactivation.	Oxborough and Baker, 1997; Ware et al., 2015
F_V'/F_M'	$(F_M'1s\text{–}F_0')/F_M'1s$	Quantum yield of PSII in a light acclimated state	van Kooten and Snel, 1990
k_D		Rate constant for deexcitation through heat dissipation	Klughammer and Schreiber, 2008
k_f		Rate constant for deexcitation through fluorescence	Klughammer and Schreiber, 2008
k_{npq}		Rate constant for deexcitation through regulated non-photochemical quenching	Klughammer and Schreiber, 2008
k_P		Rate constant for deexcitation through photochemical quenching	Genty et al., 1989
NPQ	$(F_M\text{-}F_M')/F_M'$	Stern-Volmer formulation of quenched divided by remaining PSII fluorescence.	Holzwarth et al., 2013
σ_{PSII}		Effective absorption cross section, $Å^2$ photon^{-1} or A^2 PSII^{-1} for PSII photochemistry	Kolber et al., 1998
σ_{PSII}'		Effective absorption cross section, $Å^2$ photon^{-1} or A^2 PSII^{-1}, for PSII photochemistry under excitation	Kolber et al., 1998
$\sigma_{PSII}'1s$		Effective absorption cross section, $Å^2$ photon^{-1} or A^2 PSII^{-1} for PSII photochemistry 1 s after excitation	Murphy et al., 2016
σ_i	$F_V'\,2s/F_M'\,2s = F_V'\,2s/F_M'\,2s_{t=0} \times e^{(-\sigma i \times photonA2)}$	Target size, $Å^2$ photon^{-1} or A^2 PSII^{-1}, for photoinactivation of PSII	Oliver et al., 2003; Key et al., 2010; Campbell and Tyystjärvi, 2012
YNPQ	$F_S/F_M' - F_S/F_M$	Yield of Non-Photochemical Quenching of excitation	Hendrickson et al., 2004; Kramer et al., 2004; Klughammer and Schreiber, 2008
YNO	F_S/F_M	Yield of non-regulated heat dissipation of excitation	Hendrickson et al., 2004; Kramer et al., 2004; Klughammer and Schreiber, 2008
YII	$(F_M'\text{-}F_S)/F_M'$	Yield of PSII photochemistry under excitation	Genty et al., 1989
$1–q_L$	$1–\{(F_M'\text{-}F_S)/(F_M'\text{-}F_0')*(F_0'/F_S)\}$	Excitation pressure on PSII; balance between delivery of excitation and removal of electrons	Huner et al., 1998; Kramer et al., 2004

1 s dark period to allow re-opening of PSII. We estimated the fraction of closed PSII reaction centers:

$$1 - q_L = 1 - \{(F_M' - F_S)/(F_M' - F_0')*(F_0'/F_S)\}$$

(Huner et al., 1998; Kramer et al., 2004).

$1-q_L$ is a measure of the instantaneous balance of excitation vs. electron transport in the cells. Low $1-q_L$ indicates limiting or optimal light, while high $1-q_L$ indicates incoming excitation in excess of the cellular capacity for down-stream electron transport or excitation dissipation (Huner et al., 1998).

For each actinic light step we estimated F_V'/F_M' (van Kooten and Snel, 1990). For estimations of YNPQ and YNO (Hendrickson et al., 2004; Kramer et al., 2004; Klughammer and Schreiber, 2008) we used the maximum value of F_M' attained for a given sample (Serôdio et al., 2005), not necessarily the value measured after initial dark acclimation, as our F_M basis. In some cases our light response curve extended to actinic light levels high

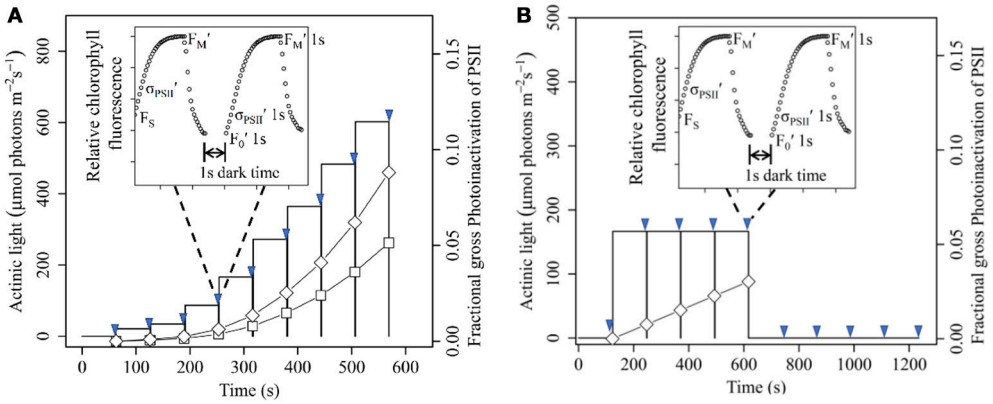

FIGURE 1 | Light Response **(A)** and Saturating Light **(B)** treatment and measuring protocols. Arrowheads show applications of repeated Fast Repetition and Relaxation chlorophyll fluorescence measurements, as shown in representative annotated inset graphs. At each measurement we applied a first fluorescence induction and relaxation in the presence of background actinic light, and then again after 1 s of dark to allow re-opening of Photosystem II. One 1 s dark intervals are indicated by vertical lines separating flashlet steps of light treatment protocols. On the right Y axis we plot the estimated gross, cumulative photoinactivation of PSII during the treatments for *Ostreococcus* (open diamonds) or *Thalassiosira* (open squares) from growth-limiting light. Net photoinactivation would be lower through PSII repair.

enough to suppress the remaining variable fluorescence to small values. When the amplitude of remaining variable fluorescence is small the reliability of the PSIWORX-R curve fitting of FRR data is poor and the resulting estimates of σ_{PSII}' suffer from wide confidence intervals. Therefore, we applied a screen to our data to exclude data points where the 95% C.I. of the estimate for σ_{PSII}' exceeded half the value of σ_{PSII}' (95% C.I./ $\sigma_{PSII}' > 0.5$). This screen excluded some points from measures of *Prochlorococcus* and *Ostreococcus* measured under high actinic light.

Using the light response curves, we chose an actinic light level at the onset of saturation which we then used to examine the induction and relaxation of YNPQ and YNO during and after short and longer exposures (**Figure 1B**) to saturating light. We set an initial dark period of either 10 or 120 s and measured the FRRf induction at the end of the dark period. Then we applied 4 sequential periods of either 10 or 120 s of the saturating actinic light at 455 nm appropriate for each species from each growth light level, with an FRRf measurement every 10 or 120 s. Then we turned off the saturating light and tracked relaxation of YNPQ under darkness with an FRRf measurement every 10 or 120 s, for a total time course of either 50 or 600 s.

A possible confounding factor in our analyses is cumulative photoinactivation of PSII during the measurement/treatment protocols (**Figure 1**) we applied to induce YNPQ. There is a long history of treating "q_I" or inhibitory quenching (Horton et al., 1996) as a component of non-photochemical quenching, in the broadest sense. Photoinactivation of PSII causes changes in PSII fluorescence emission variables, particularly increases in F_0 and F_0' (Oxborough and Baker, 1997; Ware et al., 2015) that could overlap or interfere with changes provoked by induction of YNPQ (Kulk et al., 2012, 2013). Although neither F_0 nor F_0' are explicitly included in calculation of YNPQ nor YNO, underlying changes in F_0' could shift the level of steady state fluorescence under illumination, F_S, which is part of the YNPQ and YNO parameters. We had previously determined the susceptibility of PSII to photoinactivation for each of the four taxa when grown under conditions comparable to this study (Six et al., 2009; Li and Campbell, 2013; Murphy et al., 2017) using a target size parameterization, σ_I (A^2 photon^{-1}) (Campbell and Tyystjärvi, 2012), derived from the exponential decline in PSII function plotted vs. cumulative incident photons, in the absence of PSII repair. For each treatment we therefore estimated gross cumulative photoinactivation of PSII by multiplying σ_I by cumulative photon dose imposed during during our measurement/treatment protocols to place an upper limit on the possible influences of PSII photoinactivation on the results. We furthermore compared changes in σ_{PSII}' to the sum of (YNPQ + YNO), and to the maximum quantum yield of PSII under light acclimation, F_V'/F_M', which would capture changes in photoinhibitory quenching.

We also earlier measured (Xu et al., 2017) the excitonic connectivity parameter ρ (Kolber et al., 1998; Stirbet, 2013) across the same data sets used herein. ρ measures the probability of excitation sharing among PSII centers. As some PSII close under excitation, excitation sharing under a lake model of antenna function shared across multiple reaction centers contributes to an increase in the σ_{PSII}' of the remaining open PSII. This possibility would complicate analyses of the interactions of induction of YNPQ and σ_{PSII}'. We found, however, that although ρ was significant in phytoplankters under darkness or low light, as PSII suffered closure under increasing excitation ρ dropped exponentially (Xu et al., 2017; Perkins et al., 2018). Therefore, once the phytoplankters started to induce significant YNPQ, ρ was no longer a significant factor, simplifying subsequent analyses.

Linear regressions, statistical analyses and plotting were performed using R (R Core Team, 2011) running under RStudio (RStudio Team, 2015) with the packages lsmeans (Lenth, 2016), minpack.lm (Elzhov et al., 2016), MASS (Venables and Ripley, 2002), and nlstools (Baty et al., 2015) Details of

statistical analyses are provided in figure legends and in the **Supplementary Statistical file**.

RESULTS AND DISCUSSION

In **Table 3** we present the numeric estimates for cumulative gross photoinactivation of PSII imposed during the treatments, derived using previously determined estimates of the effective absorption cross sections for photoinactivation (σ_I). Note that these numeric estimates assume no counteracting repair of PSII during treatments. This assumption is probably fulfilled for *Prochlorococcus* where instantaneous PSII repair is slow (Six et al., 2007a). *Synechococcus*, *Ostreococcus,* and *Thalassiosira* show stronger PSII repair under moderately high light (Six et al., 2007a, 2009; Li and Campbell, 2013) to counteract photoinactivation as it occurs. Therefore although these taxa incurred a metabolic burden for PSII repair (Li et al., 2015; Murphy et al., 2017) their actual net photoinhibition is much less than the gross cumulative photoinactivation, presented as an upper limit in **Table 3**.

Figure 2 plots σ_{PSII}', measured in the presence of background actinic light, vs. fractional closure of PSII (1-q_L), otherwise termed excitation pressure (Huner et al., 1998) or C (Suggett et al., 2015).

Increasing PSII closure (**Figure 2**) was driven by progressively increasing the actinic light (**Figure 1A**) applied to samples of cultures after growth under limiting or saturating light. As actinic light increases the delivery of excitation to PSII outruns down stream electron transport and an increasing fraction of PSII become closed to photochemistry. We chose to analyze responses of σ_{PSII}' measured in the presence of actinic light as our best approximation for the actual photophysiological performance of the cells. We in parallel measured σ_{PSII}' 1s determined from FRRf curves applied after 1 s of darkness following actinic light (**Figures 1A,B**, insets), to allow PSII re-opening. Although the fluorescence induction curve fitting was generally of higher quality after the 1 s re-opening, subsequent interpretations are complicated by rapid, and differential, changes in photophysiology upon the transition to darkness. In **Figure S2** we present σ_{PSII}' 1s vs. σ_{PSII}', which are indeed highly, but not perfectly, correlated.

In *Prochlorococcus* and *Synechococcus* (**Figures 2A,B**) we found higher σ_{PSII}' in cultures grown under limiting light, but no evident trends in σ_{PSII}' with PSII closure. In *Ostreococcus* (**Figure 2C**) and in *Thalassiosira* (**Figure 2D**) we found little effect of growth light upon σ_{PSII}' but a downward trend in σ_{PSII}' as PSII closure exceeded ∼0.5.

Figure 3 then plots YNPQ vs. 1-q_L determined from the same FRRf induction curves used for **Figure 2.**

The YNPQ parameter relies upon the key assumption that the rate constants for excitation decay through constitutive excitation dissipation, k_D, and for fluorescence emission, k_F, remain constant (Klughammer and Schreiber, 2008) between the measurement of F_0 or F_S at the start of the FRRf induction and the measurement of F_M or F_M' at the peak of the FRRf induction. Examination of our FRRf induction curves shows that, particularly for diatoms, the fluorescence induction curve often increases to a peak and then subsequently declines within the 128 μs FRRf flashlet train (Xu et al., 2017). Since all PSII are closed and k_P is thus driven to 0, and the flashlet intensity provoking fluorescence is constant during the flashlet train, a decrease in fluorescence implies some combination of a decrease in k_F and increases in k_D and/or k_{NPQ} as fluorescence rises from F_0 to F_M. Thus for phytoplankton rapid modulation of rate constants for excitation decay can violate an underlying assumption of the YNPQ (and the more traditional Stern-Volmer NPQ) parameters, which were originally developed for application to green plant leaves (Kramer et al., 2004; Klughammer and Schreiber, 2008) which are both optically and physiologically distinct (Chow et al., 2012) from suspensions of phytoplankton cells. Indeed recent work (Magyar et al., 2018) supports rapid changes in k_F in response to electrical effects induced within PSII during charge separation.

For both *Synechococcus* and *Thalassiosira* we saw a decrease in measured YNPQ as cells went from darkness to low light. In *Synechococcus* this dark to light decrease in measured YNPQ reflects a transition from State II to State I (Campbell and Oquist, 1996; Campbell et al., 1998) and corresponds to some increase in σ_{PSII}' (**Figure 2B**). Diatoms are thought to lack state transitions (Owens, 1986) and the decrease in YNPQ from dark to low light in *Thalassiosira* is interpreted as relaxation of a phase of non-photochemical quenching present in the dark. This "sustained NPQ" is believed to be similar to that reported in higher plants, in that it depends on the maintenance of de-epoxidized xanthophyll (diatoxanthin-DT in diatoms) that keeps the PSII antenna in a dissipative state, independent of the instantaneous transthylakoidal proton gradient (Verhoeven, 2014). A molecular mechanism for the sustained fraction of NPQ in diatoms has been proposed (Lavaud and Goss, 2014), although debate over mechanism(s) continues (Giovagnetti and Ruban, 2016) and the relative importance of multiple processes likely varies across taxa (Lavaud and Lepetit, 2013; Goss and Lepetit, 2015; Lavaud et al., 2016). Sustained NPQ is found particularly in high light acclimated diatom cells and it depends on the maintenance of a high DT pool in the dark, which we indeed observe here in *Thalassiosira* (compare limiting and saturating light grown cells in **Figure 3D** and the second derivative spectra in **Figures S3A,B**).

To separate the dark-to-light decrease in YNPQ from any subsequent increase in YNPQ as 1-q_L moved above a threshold level, we fit the data in **Figure 3** with segmented linear regressions. With these plots we sought to determine whether induction of YNPQ correlated with a given threshold of PSII closure, represented by the X intercept of the rising phase. *Ostreococcus*, from growth-saturating light, showed a 1-q_L threshold for induction of YNPQ well below the induction thresholds from growth-limiting light (**Figure 3C**), or for *Thalassiosira* from growth-saturating or growth-limiting light (**Figure 3D**) (Statistics, **Figure S3**). Thus growth saturating light induces a more sensitive induction of YNPQ in response to PSII closure in *Ostreococcus*, but not in the diatom *Thalassiosira*. Interestingly, a similar value for the induction threshold for

TABLE 3 | Predicted Photosystem II Photoinactivation during Light Treatments.

Species	Growth light	σ_I (A^2 photon^{-1})	Cumulative gross PSII photoinactivation during treatment (%)	
			Light response curve	Saturating light incubation (480 s)
Prochlorococcus	Limiting*	1.3×10^{-4} (Murphy et al., 2017)	12	1
	Saturating**	1.3×10^{-4} (Murphy et al., 2017)	7	1
Synechococcus	Limiting	1.6×10^{-4} (Murphy et al., 2017)	15	1
	Saturating	0.7×10^{-4} (Murphy et al., 2017)	17	2
Ostreococcus	Limiting	1.2×10^{-4} (Six et al., 2009)	9	1
	Saturating	n.d.	9	1
Thalassiosira	Limiting	0.7×10^{-4} (Li and Campbell, 2013)	5	0.5
	Saturating	0.8×10^{-4} (Li and Campbell, 2013)	6	0.5

*Limiting growth light, (30 μmol photons m^{-2} s^{-1}); **Saturating growth light (260 μmol photons m^{-2} s^{-1}).

non-photochemical quenching at closure of ∼0.45 of PSII has been reported in the diatom *Phaeodactylum tricornutum* grown under low light (Ruban et al., 2004; Lavaud et al., 2007). The threshold level of 1-q_L at which induction of YNPQ begins correlates well with the thresholds for light saturation of PSII electron transport, E_K, determined for the respective cultures (Xu et al., 2017). This induction threshold feature is not observed in all diatoms (i.e., *Skeletonema costatum*) and and may relate to differences in photophysiological adaptation to contrasting natural light climates (Lavaud and Lepetit, 2013; Lavaud et al., 2016).

Above this PSII closure threshold for induction of non-photochemical quenching, the slope of the rising phase of the regression then represents the sensitivity of induction of YNPQ to further progressive closure of PSII. In the study strain of *Prochlorococcus* we found a modest increase in measured YNPQ under high excitation pressure (**Figure 3A**), coinciding with the accumulation of significant predicted photoinactivation in the cultures (**Table 3**). Some strains of *Prochlorococcus* (Bailey et al., 2005; Kulk et al., 2012, 2013) have shown non-photochemical quenching phases whose induction and relaxation show temperature responses consistent with a dependence upon enzyme kinetics or membrane fluidity, which is not expected for a non-photochemical quenching response based upon photoinactivation of PSII.

We found that slopes of induction of YNPQ vs. 1-q_L for *Synechococcus*, *Ostreococcus*, and *Thalassiosira* were significantly higher for cultures from growth-saturating light than for cultures from growth-limiting light (Statistics, **Figure S3**). Thus growth saturating light induces a stronger response of YNPQ induction to progressive PSII closure across the taxa; *Synechoccoccus* had the lowest induction slope, while *Thalassiosira* from growth saturating light had the highest induction slope, once 1-q_L exceeded the induction threshold.

The stronger response of YNPQ induction in *Synechococcus* from growth saturating light (**Figure 3B**) likely represents a larger capacity for induction of non-photochemical quenching mediated by the Orange Carotenoid Protein (Boulay et al., 2008; Kirilovsky and Kerfeld, 2013; Kirilovsky, 2015). Whole cell spectra of our *Synechococcus* cultures indeed show changes in the region of 496 nm (Wilson et al., 2008), suggesting accumulation of activated Orange Carotenoid Protein of cultures from growth saturating light (**Figure S4**). We measured the induction of YNPQ under blue actinic and measuring light, absorbed primarily through chlorophyll. Cyanobacteria show stronger variations in YNPQ measured using light absorbed through the phycobilisome (Gorbunov et al., 2011) or through carotenoids (Zakar et al., 2016).

In *Ostreococcus* and *Thalassiosira* the stronger response of YNPQ induction in cells from growth saturating light (**Figures 3C,D**) likely results from a higher content of xanthophyll cycle pigments. Indeed, for the second derivative of whole cell spectra, we found a difference at 487 nm before and after 8 min of actinic light treatment in *Ostreococcus* from growth saturating light (**Figure S5B**), likely reflecting an increase in the de-epoxidised xanthophyll cycle pigment content zeaxanthin (485 nm) (Méléder et al., 2013; Ni et al., 2017). This light-dependent difference at 487 nm was not found in *Ostreococcus* from growth limiting light (**Figure S5A**), reflecting a smaller content of xanthophyll cycle pigments. We also found that the second derivative of whole cell spectra at 508 nm (Jesus et al., 2008) was different before and after actinic light treatment in *Thalassiosira* from growth saturating light, again likely reflecting an increase in the deepoxidized xanthophyll cycle pigment DT. We can attribute the spectral shift to an increase in the DT/DD ratio because the inhibitor dithiothreitol (Bachmann et al., 2004) blocks the response (**Figure S3B**).

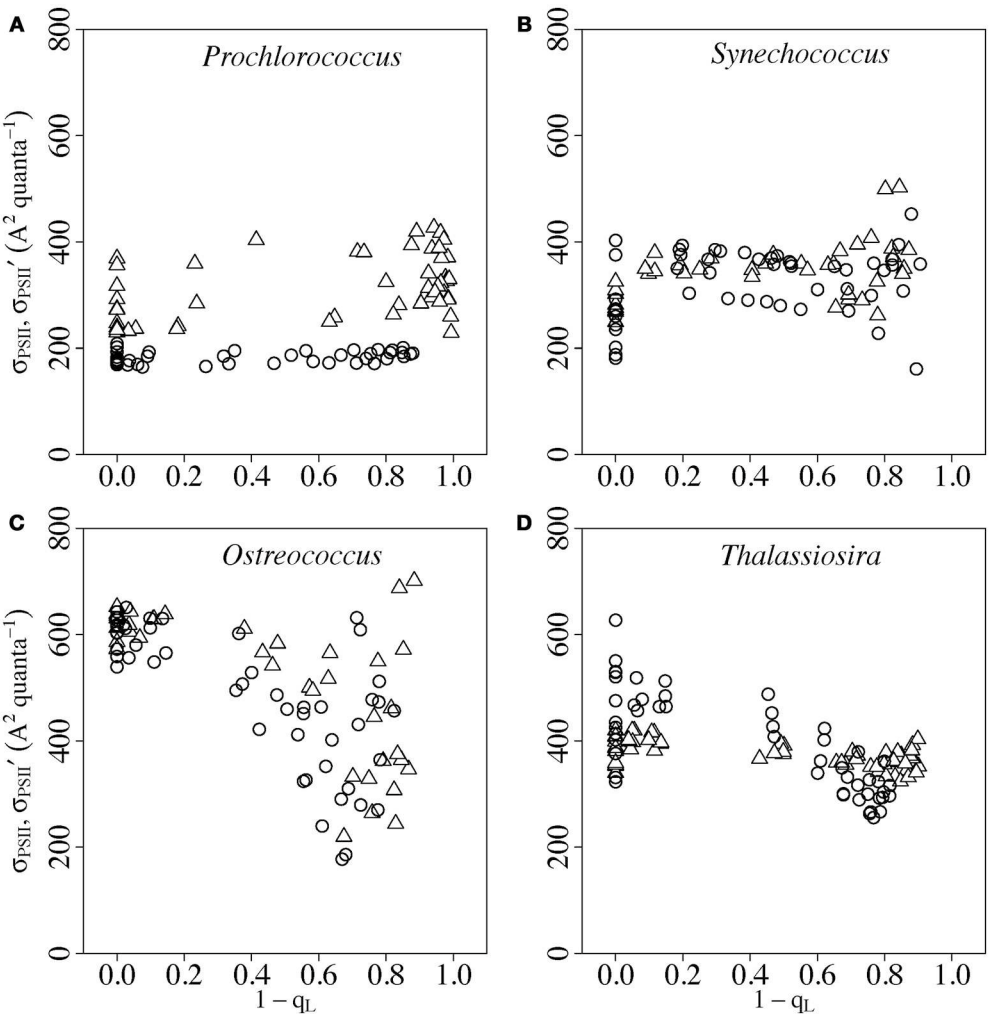

FIGURE 2 | Response of σ_{PSII}' to progressive closure of Photosystem II (1-q_L) in *Prochlorococcus* **(A)**, *Synechococcus* **(B)**, *Ostreococcus* **(C)** or *Thalassiosira* **(D)** from growth-limiting (open triangles) or growth saturating light (open circles). Photosystem II closure was driven by increasing actinic light (**Figure 1A**). Paired determinations from 4 to 8 replicate cultures plotted individually.

Figure 4 presents the responses of σ_{PSII}' to the induction of YNPQ driven by increasing actinic light (**Figure 1A**).

For the purposes of these analyses of σ_{PSII}' vs. YNPQ, we excluded the points measured under darkness, to remove effects of state transitions and/or relaxation of YNPQ from darkness to low light (**Figures 2**, **3**). In *Prochlorococcus* from growth-limiting light (**Figure 4A**), the induction of measured YNPQ reached ∼0.3. This magnitude of YNPQ was sufficient to cause a detectable down-regulation of σ_{PSII}' in *Ostreococcus* and *Thalassiosira* (**Figures 4C,**D), but in *Prochlorococcus* we found no significant down-regulation of σ_{PSII}' with light induction of YNPQ even when the actinic light reached as high as 1,600 μmol photons $m^{-2}s^{-1}$. Therefore, whatever the underlying mechanism(s) (Bailey et al., 2005; Kulk et al., 2012, 2013), we find that changes in measured YNPQ were ineffective in altering σ_{PSII}' in our studied strain of *Prochlorococcus*, measured with light absorbed through divinyl chl a. Indeed the relatively stable light and low nutrient regimes typical for *Prochlorococcus* strains argue against a large, rapidly regulated capacity for changes in excitation dissipation (Bailey et al., 2005) since it is more economical, in terms of N resource, to slowly regulate the content of antenna complexes to tune σ_{PSII} to a prevailing stable light regime, through changes in gene expression within a strain or changes in genomic encoded capacities among ecotypes (Rocap et al., 2003). Given the significant expected photoinactivation of PSII (**Table 3**) imposed by our light response treatment protocol we suggest that net photoinhibition dominated our measurements of YNPQ in this strain of *Prochlorococcus*.

In *Synechococcus* (**Figure 4B**) we found no significant down-regulation of σ_{PSII}' in response to the modest increase in YNPQ induced by increasing actinic blue light. *Synechococcus* WH 8102 does contain the Orange Carotenoid Protein (**Figure S3**) that mediates an established mechanism of non-photochemical quenching of phycobilisome excitation transfer (Wilson et al.,

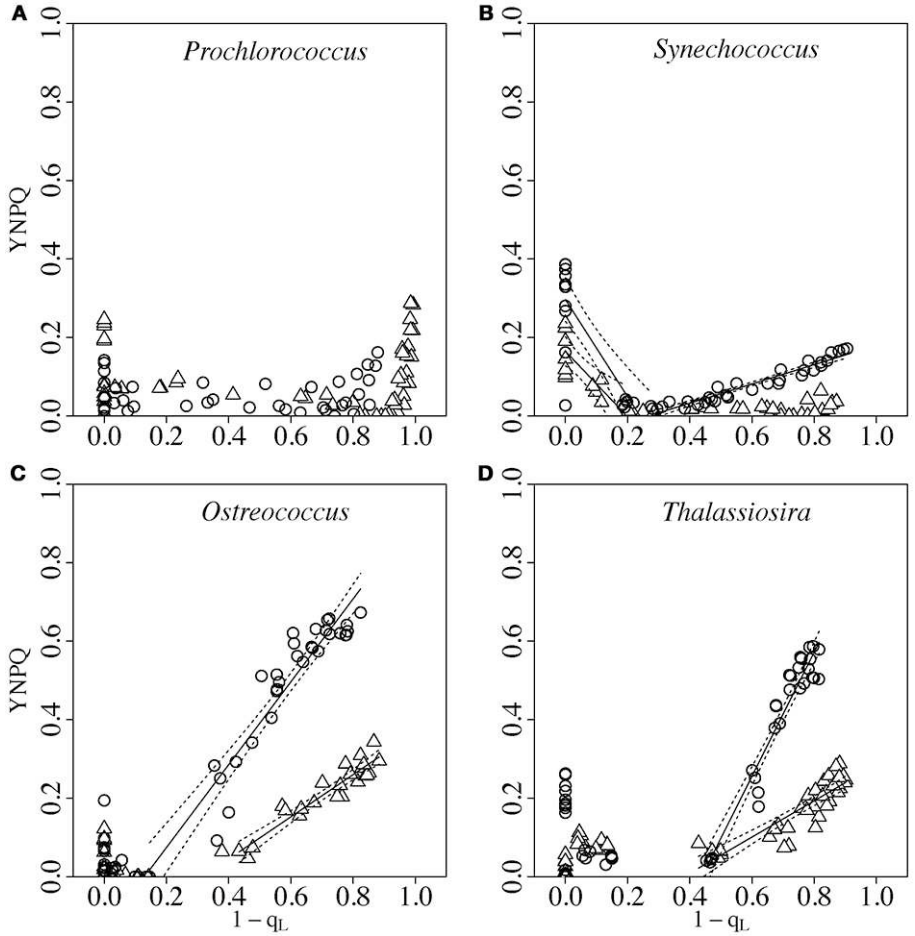

FIGURE 3 | Response of YNPQ to progressive closure of Photosystem II (1-q_L) in *Prochlorococcus* **(A)**, *Synechococcus* **(B)**, *Ostreococcus* **(C)** or *Thalassiosira* **(D)** from growth-limiting (open triangles) or growth saturating light (open circles). Photosystem II closure was driven by increasing actinic light (**Figure 1A**). Paired determinations from 4 to 8 replicate cultures plotted individually. Solid lines show segmented linear regressions to determine the break point for induction of YNPQ and the response of YNPQ to increasing Photosystem II closure. Dotted lines show 95% C.I. on the regression lines.

2007; Boulay et al., 2008; Gorbunov et al., 2011; Kirilovsky and Kerfeld, 2013; Kirilovsky, 2015). But under our growth and blue light treatment conditions, the YNPQ induction in *Synechococcus* was insufficient to cause a detectable down-regulation of σ_{PSII}'. Note that **Figure 4B** excludes data points measured in darkness, where transition to State II does indeed cause a significant increase in measured YNPQ (Campbell et al., 1998) and a parallel detectable dark down-regulation of σ_{PSII}' (**Figure 2B**). Therefore, our lack of response of σ_{PSII}' to induction of YNPQ in *Synechococcus* under excess light was not a matter of analytical insensitivity. We find that YNPQ reflects at least two distinct processes in *Synechococcus*. We found an increase in σ_{PSII}' (**Figure 2B**) during a dark to light transition, in parallel with simultaneous down-regulation of measured YNPQ (**Figure 3B**). In contrast we found a lack of response of σ_{PSII}' to a comparable magnitude of YNPQ induction under excess blue light (**Figure 4B**). Our measures under 455 nm blue light, delivered to the small chl a absorption cross section associated with cyanobacterial PSII, largely bypass mechanisms including the Orange Carotenoid Protein that modulate excitation delivery through the phycobilisome (Gorbunov et al., 2011; Zakar et al., 2016), which could generate detectable changes in σ_{PSII}'.

In *Ostreococcus* (**Figure 4C**) cultures from growth-limiting or growth-saturating light showed a common Y-axis intercept, showing no significant acclimatory change in σ_{PSII} between the two growth light intensities. Data for *Ostreococcus* then fell upon a common regression of down regulation of σ_{PSII}' with increasing YNPQ (Statistics, **Figure S4**). In *Thalassiosira* (**Figure 4D**) the cultures from growth-saturating light actually showed a slightly higher initial σ_{PSII} Y intercept. Cultures from growth limiting or growth saturating light then fell upon a common regression slope of down-regulation of σ_{PSII}' with increasing YNPQ (Statistics, **Figure S4**). The higher initial σ_{PSII} Y intercept for *Thalassiosira* from growth saturating light is attributable to the relaxation of the sustained NPQ which was stronger in cultures from growth-saturating light (see **Figure 3D**). It is noteworthy that σ_{PSII}' measured under high actinic light showed high variability and wide confidence

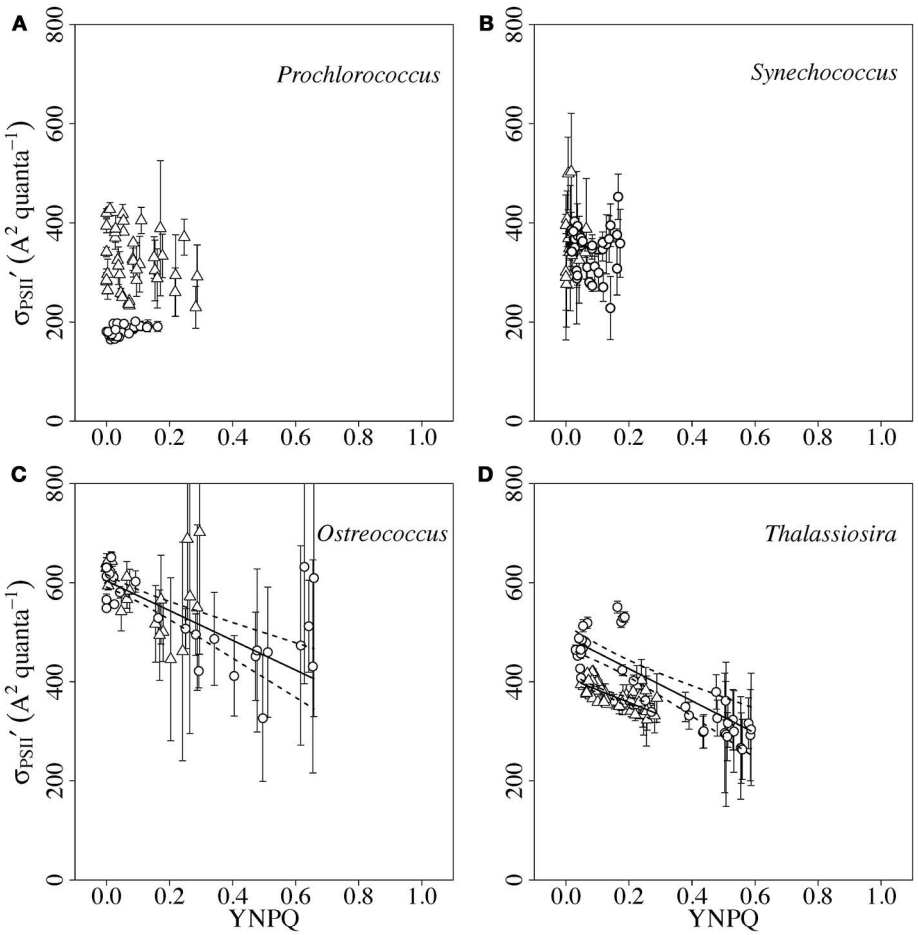

FIGURE 4 | σ_{PSII}' vs. YNPQ in *Prochlorococcus* **(A)**, *Synechococcus* **(B)**, *Ostreococcus* **(C)** or *Thalassiosira* **(D)** from growth-limiting (open triangles) or growth saturating light (open circles). Induction of YNPQ was driven by increasing actinic light (**Figure 1A**). Paired determinations from 4 to 8 replicate cultures plotted individually. Solid lines show linear regressions; dotted lines show 95% C.I. on the regression lines.

intervals, since the amplitude of variable fluorescence remaining above steady state fluorescence was small (Xu et al., 2017). In **Figure S6** we give the analogous plots of σ_{PSII}' 1s with increasing YNPQ 1s, which support the same interpretations, consistent with the strong correlation of σ_{PSII}' 1s vs. σ_{PSII}' (**Figure S2**). The exception is that after 1s darkness *Synechococcus* shows a correlation between downregulation of σ_{PSII}' 1s and the induction of YNPQ. We attribute this to the rapid transition from State I (light) to down regulated State II (dark) (Campbell et al., 1998).

The YNO yield parameterizes non-regulated excitation dissipation through the thermal deexcitation, k_D, and fluorescence emission, k_F, excitation decay rate constants (Kramer et al., 2004; Klughammer and Schreiber, 2008). We plotted σ_{PSII}' vs. (YNPQ + YNO) (**Figure 5**) but found, as expected, that the plots showed weaker correlations than equivalent plots of σ_{PSII}' vs. YNPQ, so that YNO had no additional power to explain changes in σ_{PSII}'. Indeed at least in diatoms the induction of YNPQ suppresses YNO (Perkins et al., 2018), so the measures tend to anti-correlate. Since YNO parameterizes processes largely mediated through the PSII reaction center it is reasonable that it has little influence upon σ_{PSII}'.

To compare whether light induction of YNPQ had a proportional effect upon down regulation of σ_{PSII}' we normalized σ_{PSII}' to the Y intercept of the regression of σ_{PSII}' vs. YNPQ (**Figure 4**) for each available combination of taxa and growth light (**Figure 5**), again excluding data points measured in darkness.

Since *Prochlorococcus* and *Synechococcus* did not show a statistically significant regression of σ_{PSII}' vs. YNPQ under increasing light (**Figures 4A,B**) we did not perform the normalizations for those taxa. For *Ostrecococcus* (**Figure 6A**) and *Thalassiosira* (**Figure 6B**) cultures from both growth-limiting and growth-saturating light data fell upon slopes of −0.48 (−0.17 to −0.78, 95% C.I.) (*Ostreococcus*) or −0.68 (± −0.52 to −0.89, 95% C.I.) (*Thalassiosira)* for the intercept normalized σ_{PSII}' vs. YNPQ. These slopes are significantly smaller in absolute magnitude than the −1 slope expected if YNPQ induction had a directly proportional effect upon σ_{PSII}' (Statistics, **Figure S5**).

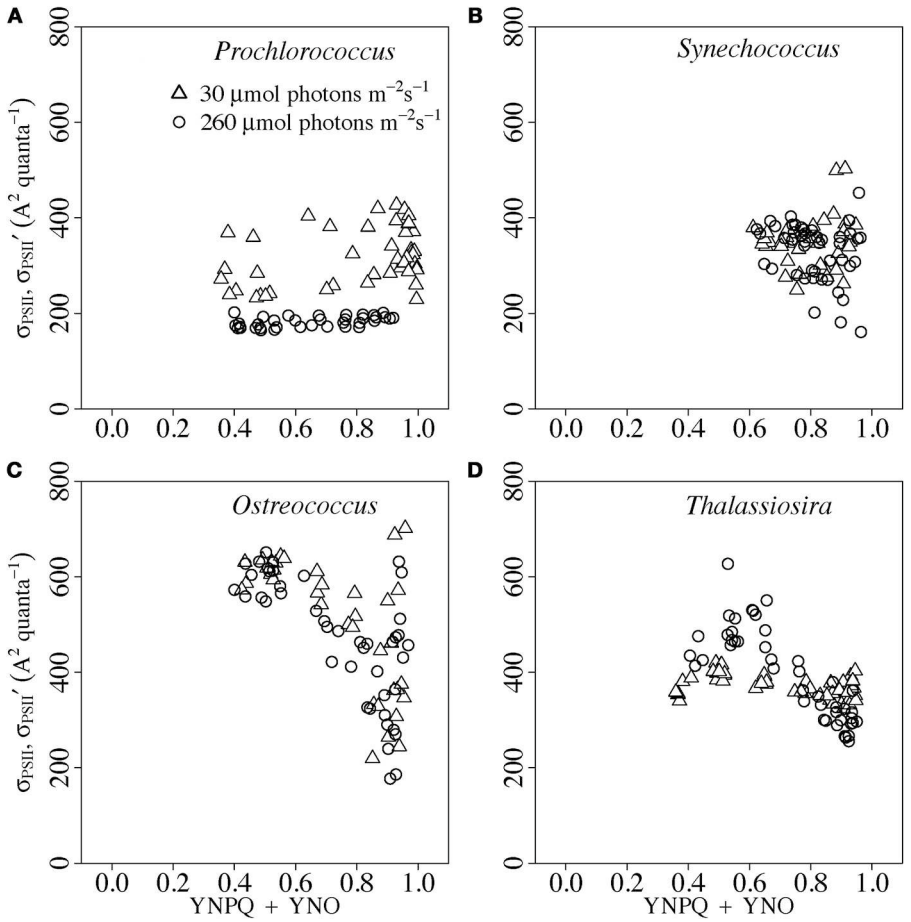

FIGURE 5 | σ_{PSII}' vs. YNO plus YNPQ in *Prochlorococcus* **(A)**, *Synechococcus* **(B)**, *Ostreococcus* **(C)**, or *Thalassiosira* **(D)** from growth-limiting (open triangles) or growth saturating light (open circles). Induction of YNO and YNPQ was driven by increasing actinic light (**Figure 1A**). Paired determinations from 4 to 8 replicate cultures plotted individually.

In two diverse eukaryotic phytoplankters the effect of measured YNPQ upon down regulation of simultaneously measured σ_{PSII}' was significant, but at less than the 1:1 proportionality expected for a yield coefficient.

We next sought to determine whether the relationship between down-regulation of σ_{PSII}' and induction of YNPQ depends upon the immediate light history of the sample, or whether the relationship is consistent across differing histories of induction and relaxation. In **Figure 7** we therefore plot intercept-normalized σ_{PSII}' vs. YNPQ for culture samples exposed to either 40 or 480 s of saturating light (open symbols) followed by dark relaxation periods (closed symbols).

In *Synechococcus* from growth-saturating light (**Figure 7A**), there was no significant down-regulation of intercept-normalized σ_{PSII}' vs. YNPQ during the saturating light incubation (open symbols). During the subsequent dark period we saw a significant down regulation of σ_{PSII}' with increasing YNPQ as the cells reverted from State I (illumination) to State II (darkness) (closed symbols) (Campbell et al., 1998).

In *Ostreococcus* (**Figure 7B**) intercept-normalized σ_{PSII}' vs. YNPQ from cultures from growth-saturating light, treated under saturating actinic light fell upon a common regression with the same cultures during dark relaxation from the saturating actinic light (Statistics, **Figure S7**). Thus, there was no hysteresis in the response of σ_{PSII}' vs. YNPQ; the immediate light history of the samples had no significant influence upon a consistent downregulation of σ_{PSII}' with increasing YNPQ. Furthermore, the slope of the common regression (**Figure 7B**) was not significantly different from that found in **Figure 6A** for *Ostreococcus* exposed to progressively increasing light (Statistics, **Figure S6**). Finally, cultures from growth-limiting or growth saturating light (**Figure 6A**) fell upon the same common regression, so longer term light acclimatory history had no significant effect upon the relation between σ_{PSII}' with increasing YNPQ in *Ostreococcus.*

Similarly, in *Thalassiosira* (**Figure 7C**) intercept-normalized σ_{PSII}' vs. YNPQ from cultures from growth-saturating light, treated under saturating actinic light fell upon a common regression with the same cultures during dark relaxation from saturating actinic light (Statistics, **Figure S6**). This common regression was not significantly different from the regression observed from cultures under progressively

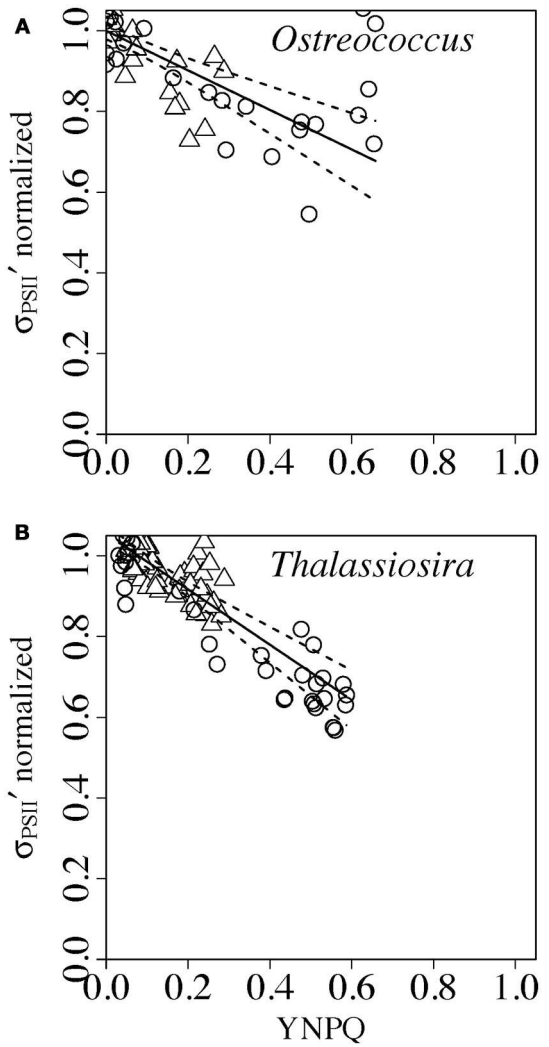

FIGURE 6 | Normalized σ_{PSII}' vs. YNPQ in *Ostreococcus* **(A)** or *Thalassiosira* **(B)** from growth-limiting (open triangles) or growth saturating light (open circles). Induction of YNPQ was driven by increasing actinic light (**Figure 1A**). σ_{PSII}' was normalized to the regression intercept for a particular data set (**Figure 4**) to scale change in σ_{PSII}' from 1 to 0. Paired determinations from 4 to 8 replicate cultures plotted individually. Solid lines show linear regressions; dotted lines show 95% C.I. on the regression lines.

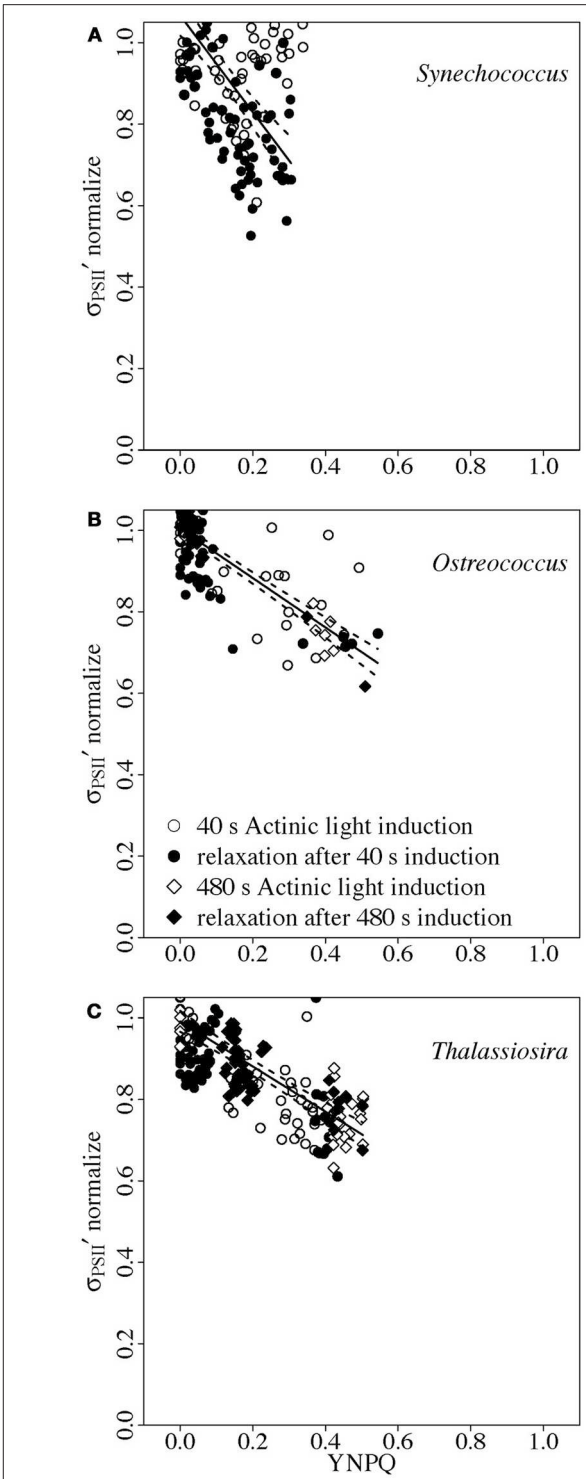

FIGURE 7 | Normalized σ_{PSII}' vs. YNPQ in *Synechococcus* **(A)**, *Ostreococcus* **(B)**, or *Thalassiosira* **(C)** from growth saturating light. Induction of YNPQ was driven by a time course exposure to saturating light (open symbols) for 40 s (circles) or 480 s (diamonds) (**Figure 1B**). Subsequent relaxation of YNPQ was thereafter tracked in darkness (**Figure 1B**) (closed symbols). σ_{PSII}' was normalized to the regression intercept for a particular data set to scale change in σ_{PSII}' from 1 to 0. Paired determinations from 4 to 8 replicate cultures plotted individually. Solid lines show linear regressions; dotted lines show 95% C.I. on the regression lines.

increasing light (**Figure 6B**), and cultures from growth-limiting or growth-saturating light fell upon the common regression (**Figure 6B**) (Statistics, **Figure S6**). Thus in both *Ostreococcus* or in *Thalassiosira* a given level of YNPQ imposes a consistent down-regulation upon σ_{PSII}' within a given taxa, whatever the preceding light history. This likely reflects the fundamental commonalities in a YNPQ parameter dominated by xanthophyll mediated quenching in both *Ostreococcus* or in *Thalassiosira*. Maximum photoinhibition of PSII was small (less than 9%) under our treatments of these two eukaryotic taxa (**Table 3**), so any influence of photoinhibition upon YNPQ was negligible.

It is noteworthy that the prokaryotic *Synechococcus* does show a hysteresis in the relation between measured YNPQ and down-regulation of σ_{PSII}' under blue light depending upon whether the

measured YNPQ reflects a dark to light state transition, or an induction under high light attributable to the orange-carotenoid protein (Boulay et al., 2008).

If the regression line for σ_{PSII}' vs. YNPQ in *Ostreococcus* (**Figure 4C**) is extrapolated out to a maximum YNPQ = 1 the residual σ'_{PSII}~286 A^2 $PSII^{-1}$, while the equivalent extrapolation to YNPQ = 1 gives a residual σ'_{PSII}~167 A^2 $PSII^{-1}$ for *Thalassiosira* (**Figure 4D**). In fact, across our studies to date (Ni et al., 2017; **Figure S7**) the maximum YNPQ we have consistently observed is ~0.6 in an arctic strain of the prasinophyte *Micromonas*. As a conceptual exercise we used the chlorophyll-specific absorption coefficient, corrected for cell size (Fujiki and Taguchi, 2002), and the 35 chlorophyll content of the core of PSII (Umena et al., 2011) to estimate the approximate effective absorption cross section for PSII in the absence of any associated antenna complexes. For *Ostreococcus* we estimate a minimal effective absorption cross section of ~96 A^2 $PSII^{-1}$ for the 35 chlorophylls of the PSII core complex, at our measurement light of 455 nm. The larger *Thalassiosira* suffers somewhat more optical screening through pigment packaging effects (Fujiki and Taguchi, 2002) and we estimate a minimal effective absorption cross section of ~79 A^2 $PSII^{-1}$. These estimates are 1/3–1/2 the size of the residual σ_{PSII}' estimated from regression out to YNPQ = 1. Therefore there is a significant residual pigment bed serving PSII, functionally equivalent to ~74–104 chlorophylls that is not regulated by any degree of measured YNPQ induction. These results closely parallel findings in the diatom *Phaeodactylum tricornutum* that induction of Stern-Volmer NPQ above ~1 has no further effect upon down regulation of the PSII cross section (Giovagnetti and Ruban, 2016). This in turn suggests a violation in the theoretical model supporting the extraction of the YNPQ or the σ_{PSII}' parameters. Given our observations of transient down-regulation of fluorescence emission during and immediately after FRRf flashlet trains (Xu et al., 2017) we suggest that the assumption of constant k_D and k_F required for derivation of YNPQ (Klughammer and Schreiber, 2008) can be violated in *Ostrecoccocus* and *Thalassiosira* even within the duration of an FRRf flashlet train. Experimental and theoretical work indeed supports changes in the fluorescence yield of PSII caused by transient changes in electric fields, and not directly related to photochemistry nor to non-photochemical dissipation of excitation (Magyar et al., 2018).

CONCLUSIONS

Measures of non-photochemical quenching of chlorophyll fluorescence are widely used to infer changes in excitation allocation and photoprotection in phytoplankters. In parallel σ_{PSII} from dark-acclimated cells or σ_{PSII}' from light-acclimated cells are used to estimate photoacclimation status and electron transport rates.

In a strain of *Prochlorococcus* we measured induction of low levels of YNPQ, probably attributable to cumulative photoinactivaton of PSII, which had no significant effect upon σ_{PSII}'. In a strain of marine *Synechococcus* we found inductions of YNPQ under excess blue light, attributable to accumulation of activated Orange Carotenoid Protein, but again did not find a significant down-regulation of σ_{PSII}' under excess blue light delivered directly to PSII. At similar levels of measured YNPQ in darkness we did find a detectable down-regulation of σ_{PSII}' due to a state transition in *Synechococcus*. Thus for the two prokaryotes, detectable changes in YNPQ under excess blue light were not correlated with down regulation of σ_{PSII}', but we did detect correlated changes in YNPQ and σ_{PSII}' during dark to light state transitions.

In the chl a/b Prasinophyte phytoplankter *Ostreococcus* we found a significant induction of YNPQ with progressive closure of PSII. Growth under saturating light lowered the threshold for this induction of YNPQ and increased the subsequent induction slope, attributable to a higher content of xanthophyll cycle pigments. In the chl a/c diatom *Thalassiosira* we also found significant induction of YNPQ with progressive closure of PSII above a threshold. Growth under saturating light increased the induction slope, again attributable to a higher content of xanthophyll cycle pigments.

Within the tested eukaryotic taxa the supposed yield co-efficient for non-photochemical quenching, YNPQ, correlates with a consistent down-regulation of σ_{PSII}', but it does not provoke a 1:1 down regulation of σ_{PSII}' in either taxon, and significant residual σ_{PSII}' remains even under a hypothetical maximum induction of YNPQ = 1. The discrepancy is even larger between the down regulation of σ_{PSII}' and induction of the unbounded Stern-Volmer NPQ parameter (Giovagnetti and Ruban, 2016; **Figure S1**). The relation between a given level of YNPQ and a given down-regulation of σ_{PSII}' was however consistent across different short- and long-term light histories for both *Ostrecococcus* and *Thalassiosira*.

The light threshold and magnitude of induction of YNPQ in relation to incident light or PSII closure changes with acclimation state. For representative eukaryotic taxa we can predict changes in σ_{PSII}', useful for modeling acclimation or marine productivity (Suggett et al., 2009), from measures of YNPQ (Kramer et al., 2004; Klughammer and Schreiber, 2008) which are accessible from fluorescence measures that do not include σ_{PSII}'. This useful relation does not generally extend to the tested prokaryotes, at least for blue light. We sound caution on interpreting induction of YNPQ in terms of a directly proportional down-regulation of delivery of excitation to PSII as measured by σ_{PSII}'. The significant residual σ_{PSII}' at maximum YNPQ shows that a fraction of the light harvesting capacity serving PSII, measured through σ_{PSII}', is not subject to downregulation through the process(es) that drive measured YNPQ.

SUMMARY

σ_{PSII} shows differing responses to YNPQ, depending upon phytoplankter taxa.

AUTHOR CONTRIBUTIONS

KX grew the cultures, conducted the experiments, generated the figures, and did the data analyses. RP and JL contributed to the data analyses, interpretation, and discussion. EA guided the statistical analyses and interpretation of the data. MB contributed

Figure S5 and contributed to discussions. DC designed the project, guided the data analyses, and wrote the draft of the manuscript with contributions from all authors.

FUNDING

This study was funded by the Natural Sciences and Engineering Research Council of Canada (DC) and the Canada Research Chairs (DC) using equipment funded by the New Brunswick Innovation Foundation (DC) and the Canada Foundation for Innovation (DC). EU Horizon 2020 No 734708/GHANA/H2020-MSCA-RISE-2016 supported the participation of JL, RP, and MB.

ACKNOWLEDGMENTS

The authors thank Jessica Grant-Burt and Miranda Corkum for assistance with scripting and culturing. Dr. C. Mark Moore, National Oceanography Centre, University of Southhampton, UK, provided generous pre-review comments on derivations of fluorescence parameters.

SUPPLEMENTARY MATERIAL

The Supplementary Material for this article can be found online at: https://www.frontiersin.org/articles/10.3389/fmars.2018.00281/full#supplementary-material

Figure S1 | NPQ vs. YNPQ in *Prochlorococcus* **(A)**, *Synechococcus* **(B)**, *Ostreococcus* **(C)**, or *Thalassiosira* **(D)** from growth-limiting (open triangles) or growth saturating light (open circles). Induction of NPQ and YNPQ was driven by increasing actinic light (**Figure 1A**). Paired determinations from 4 to 8 replicate cultures plotted individually.

Figure S2 | σ_{PSII}' 1s vs. σ_{PSII}' in *Prochlorococcus* **(A)**, *Synechococcus* **(B)**, *Ostreococcus* **(C)**, or *Thalassiosira* **(D)** from growth-limiting (open triangles) or growth saturating light (open circles). σ_{PSII}' was measured under increasing levels of actinic light (**Figure 1A**). σ_{PSII}' 1s was measured after 1 s of darkness following each actinic light level (**Figure 1A**). Paired determinations from 4 to 8 replicate cultures plotted individually.

Figure S3 | The normalized second derivative of whole cell spectra of *Thalassiosira* from growth-limiting **(A,C)** or growth saturating light **(B,D)**. Samples were treated without or with dithiothreitol (DTT) to develop or inhibit the deepoxidation of the xanthophyll cycle. The whole cell spectra were measured before (solid line) and after (dashed line) 8 min of actinic light treatment. Average of paired determinations from 2 to 3 replicate cultures plotted.

Figure S4 | The normalized second derivative of whole cell spectra of *Synechococcus* from growth-limiting (solid line) or growth saturating light (dotted line). Average of paired determinations from 2 to 3 replicate cultures plotted.

Figure S5 | The normalized second derivative of whole cell spectra of *Ostreococcus* from growth-limiting **(A,C)** or growth saturating light **(B,D)**. Samples were treated without or with dithiothreitol (DTT) to develop or inhibit the deepoxidation of the xanthophyll cycle. The whole cell spectra were measured before (solid line) and after (dashed line) 8 min of actinic light treatment. Average of paired determinations from 2 to 3 replicate cultures plotted.

Figure S6 | σ_{PSII}' 1s vs. YNPQ 1s in *Prochlorococcus* **(A)**, *Synechococcus* **(B)**, *Ostreococcus* **(C)**, or *Thalassiosira* **(D)** from growth-limiting (open triangles) or growth saturating light (open circles). Induction of YNPQ 1s was driven by increasing actinic light (**Figure 1A**). Paired determinations from 4 to 8 replicate cultures plotted individually. Solid lines show linear regressions; dotted lines show 95% C.I. on the regression lines.

Figure S7 | σ_{PSII}' vs. YNPQ in **(A)** in *Chlorella vulgaris*, **(B)** *Haslea ostrearia*, **(C)** *Haslea* sp. (Indonesian strain), or **(D)** *Micromonas* NCMA 2099 (arctic strain growing at 2C). Induction of YNPQ was driven by increasing actinic light. Paired determinations from 3 to 15 cultures of each strain plotted individually and fitted with a linear regression (solid line); 95% C.I. on the regression shown by dotted lines.

REFERENCES

Bachmann, K. M., Ebbert, V., Adams, W. W. III., Verhoeven, A. S., Logan, B. A., and Demmig-Adams, B. (2004). Effects of lincomycin on PSII efficiency, non-photochemical quenching, D1 protein and xanthophyll cycle during photoinhibition and recovery. *Funct. Plant Biol.* 31, 803–813. doi: 10.1071/FP04022

Bailey, S., Mann, N. H., Robinson, C., and Scanlan, D. J. (2005). The occurrence of rapidly reversible non-photochemical quenching of chlorophyll *a* fluorescence in cyanobacteria. *FEBS Lett.* 579, 275–280. doi: 10.1016/j.febslet.2004.11.091

Baty, F., Ritz, C., Charles, S., Brutsche, M., Flandrois, J.-P., and Delignette-Muller, M.-L. (2015). A toolbox for nonlinear regression in R: the package nlstools. *J. Stat. Softw.* 66, 1–21. doi: 10.18637/jss.v066.i05

Boulay, C., Abasova, L., Six, C., Vass, I., and Kirilovsky, D. (2008). Occurrence and function of the orange carotenoid protein in photoprotective mechanisms in various cyanobacteria. *Biochim. Biophys. Acta* 1777, 1344–1354. doi: 10.1016/j.bbabio.2008.07.002

Campbell, D. A., and Tyystjärvi, E. (2012). Parameterization of photosystem II photoinactivation and repair. *Biochim. Biophys. Acta* 1817, 258–265. doi: 10.1016/j.bbabio.2011.04.010

Campbell, D., Hurry, V., Clarke, A. K., Gustafsson, P., and Öquist, G. (1998). Chlorophyll fluorescence analysis of cyanobacterial photosynthesis and acclimation. *Microbiol. Mol. Biol. Rev.* 62, 667–683.

Campbell, D., and Oquist, G. (1996). Predicting light acclimation in *Cyanobacteria* from nonphotochemical quenching of photosystem II fluorescence, which reflects state transitions in these organisms. *Plant Physiol.* 111, 1293–1298.

Chow, W. S., Fan, D. Y., Oguchi, R., Jia, H., Losciale, P., Park, Y. I., et al. (2012). Quantifying and monitoring functional photosystem II and the stoichiometry of the two photosystems in leaf segments: approaches and approximations. *Photosynth. Res.* 113, 63–74. doi: 10.1007/s11120-012-9740-y

Chrétiennot-Dinet, M.-J., Courties, C., Vaquer, A., Neveux, J., Claustre, H., Lautier, J., et al. (1995). A new marine picoeucaryote: *Ostreococcus tauri* gen. et sp. nov. (Chlorophyta, Prasinophyceae). *Phycologia* 34, 285–292. doi: 10.2216/i0031-8884-34-4-285.1

Elzhov, T. V., Mullen, K. M., Spiess, A.-N., and Bolker, B. (2016). *minpack.lm: R Interface to the Levenberg-Marquardt Nonlinear Least-Squares Algorithm Found in MINPACK, Plus Support for Bounds*. Available online at: https://CRAN.R-project.org/package=minpack.lm

Falkowski, P. G., and Owens, T. G. (1980). Light–shade adaptation 1. *Plant Physiol.* 66, 592–595.

Fujiki, T., and Taguchi, S. (2002). Variability in chlorophyll a specific absorption coefficient in marine phytoplankton as a function of cell size and irradiance. *J. Plankton Res.* 24, 859–874. doi: 10.1093/plankt/24.9.859

Genty, B., Briantais, J.-M., and Baker, N. R. (1989). The relationship between the quantum yield of photosynthetic electron transport and quenching of chlorophyll fluorescence. *Biochim. Biophys. Acta* 990, 87–92. doi: 10.1016/S0304-4165(89)80016-9

Giovagnetti, V., and Ruban, A. V. (2016). Detachment of the fucoxanthin chlorophyll a/c binding protein (FCP) antenna is not involved in the acclimative regulation of photoprotection in the pennate diatom *Phaeodactylum tricornutum*. *Biochim. Biophys. Acta.* 1858, 218–230. doi: 10.1016/j.bbabio.2016.12.005

Gorbunov, M. Y., Kuzminov, F. I., Fadeev, V. V., Kim, J. D., and Falkowski, P. G. (2011). A kinetic model of non-photochemical quenching in cyanobacteria. *Biochim. Biophys. Acta* 1807, 1591–1599. doi: 10.1016/j.bbabio.2011.08.009

Goss, R., and Lepetit, B. (2015). Biodiversity of NPQ. *J. Plant Physiol.* 172, 13–32. doi: 10.1016/j.jplph.2014.03.004

Hendrickson, L., Furbank, R. T., and Chow, W. S. (2004). A simple alternative approach to assessing the fate of absorbed light energy using chlorophyll fluorescence. *Photosynth. Res.* 82, 73–81. doi: 10.1023/B:PRES.0000040446.87305.f4

Holzwarth, A. R., Lenk, D., and Jahns, P. (2013). On the analysis of non-photochemical chlorophyll fluorescence quenching curves. *Biochim. Biophys. Acta* 1827, 786–792. doi: 10.1016/j.bbabio.2013.02.011

Horton, P., Ruban, A. V., and Walters, R. G. (1996). Regulation of light harvesting in green plants. *Annu. Rev. Plant Physiol. Plant Mol. Biol.* 47, 655–684. doi: 10.1146/annurev.arplant.47.1.655

Huner, N. P., Öquist, G., and Sarhan, F. (1998). Energy balance and acclimation to light and cold. *Trends Plant Sci.* 3, 224–230. doi: 10.1016/S1360-1385(98)01248-5

Ito, H., and Tanaka, A. (2011). Evolution of a divinyl chlorophyll-based photosystem in *Prochlorococcus*. *Proc. Natl. Acad. Sci. U.S.A.* 108, 18014–18019. doi: 10.1073/pnas.1107590108

Jesus, B., Mouget, J.-L., and Perkins, R. G. (2008). Detection of diatom xanthophyll cycle using spectra reflectance. *J. Phycol.* 44, 1349–1359. doi: 10.1111/j.1529-8817.2008.00583.x

Key, T., Mccarthy, A., Campbell, D., Six, C., Roy, S., and Finkel, Z. (2010). Cell size trade-offs govern light exploitation strategies in marine phytoplankton. *Environ. Microbiol.* 12, 95–104. doi: 10.1111/j.1462-2920.2009.02046.x

Kirilovsky, D. (2015). Modulating energy arriving at photochemical reaction centers: orange carotenoid protein-related photoprotection and state transitions. *Photosynth. Res.* 126, 3–17. doi: 10.1007/s11120-014-0031-7

Kirilovsky, D., and Kerfeld, C. A. (2013). The orange carotenoid protein: a blue-green light photoactive protein. *Photochem. Photobiol. Sci.* 12, 1135–1143. doi: 10.1039/c3pp25406b

Klughammer, C., and Schreiber, U. (2008). Complementary PS II quantum yields calculated from simple fluorescence parameters measured by PAM fluorometry and the Saturation Pulse method. *PAM Appl. Notes* 1, 27–35.

KoblíŽek, M., Kaftan, D., and Nedbal, L. (2001). On the relationship between the non-photochemical quenching of the chlorophyll fluorescence and the Photosystem II light harvesting efficiency. A repetitive flash fluorescence induction study. *Photosynth. Res.* 68, 141–152. doi: 10.1023/A:1011830015167

Kolber, Z. S., Prasil, O., and Falkowski, P. G. (1998). Measurements of variable chlorophyll fluorescence using fast repetition rate techniques: defining methodology and experimental protocols. *Biochim. Biophys. Acta* 1367, 88–106. doi: 10.1016/S0005-2728(98)00135-2

Kramer, D. M., Johnson, G., Kiirats, O., and Edwards, G. E. (2004). New fluorescence parameters for the determination of Q_A redox state and excitation energy fluxes. *Photosynth. Res.* 79, 209–218. doi: 10.1023/B:PRES.0000015391.99477.0d

Kulk, G., de Vries, P., van de Poll, W., and Buma, A. G. J. (2013). "Temperature-dependent photoregulation in oceanic picophytoplankton during excessive irradiance exposure," in *Photosynthesis*, ed Z. Dubinsky (London: InTech).

Kulk, G., de Vries, P., van de Poll, W., Visser, R., and Buma, A. (2012). Temperature-dependent growth and photophysiology of prokaryotic and eukaryotic oceanic picophytoplankton. *Mar. Ecol. Prog. Ser.* 466, 43–55. doi: 10.3354/meps09898

Lambrev, P. H., Miloslavina, Y., Jahns, P., and Holzwarth, A. R. (2012). On the relationship between non-photochemical quenching and photoprotection of Photosystem II. *Biochim. Biophys. Acta* 1817, 760–769. doi: 10.1016/j.bbabio.2012.02.002

Laney, S. R. (2003). Assessing the error in photosynthetic properties determined with Fast Repetition Rate fluorometry. *Limnol. Oceanogr.* 48, 2234–2242. doi: 10.4319/lo.2003.48.6.2234

Laney, S. R., and Letelier, R. M. (2008). Artifacts in measurements of chlorophyll fluorescence transients, with specific application to fast repetition rate fluorometry. *Limnol. Oceanogr. Methods* 6, 40–50. doi: 10.4319/lom.2008.6.40

Lavaud, J., and Goss, R. (2014). "The peculiar features of non-photochemical fluorescence quenching in diatoms and brown algae," in *Non-Photochemical Quenching and Energy Dissipation in Plants, Algae and Cyanobacteria Advances in Photosynthesis and Respiration*, eds B. Demmig-Adams, G. Garab, W. A. III., and Govindjee (Dordrecht: Springer), 421–443.

Lavaud, J., and Lepetit, B. (2013). An explanation for the inter-species variability of the photoprotective non-photochemical chlorophyll fluorescence quenching in diatoms. *Biochim. Biophys. Acta* 1827, 294–302. doi: 10.1016/j.bbabio.2012.11.012

Lavaud, J., Six, C., and Campbell, D. A. (2016). Photosystem II repair in marine diatoms with contrasting photophysiologies. *Photosynth. Res.* 127, 189–199. doi: 10.1007/s11120-015-0172-3

Lavaud, J., Strzepek, R. F., and Kroth, P. G. (2007). Photoprotection capacity differs among diatoms: Possible consequences on the spatial distribution of diatoms related to fluctuations in the underwater light climate. *Limnol. Oceanogr.* 52, 1188–1194. doi: 10.4319/lo.2007.52.3.1188

Lenth, R. V. (2016). Least-squares means: the R package lsmeans. *J. Stat. Softw.* 69, 1–33. doi: 10.18637/jss.v069.i01

Li, D., Xie, J., Zhao, J., Xia, A., Li, D., and Gong, Y. (2004). Light-induced excitation energy redistribution in *Spirulina platensis* cells: "spillover" or "mobile PBSs"? *Biochim. Biophys. Acta* 1608, 114–121. doi: 10.1016/j.bbabio.2003.11.002

Li, G., Brown, C. M., Jeans, J. A., Donaher, N. A., McCarthy, A., and Campbell, D. A. (2015). The nitrogen costs of photosynthesis in a diatom under current and future pCO_2. *New Phytol.* 205, 533–543. doi: 10.1111/nph.13037

Li, G., and Campbell, D. A. (2013). Rising CO_2 interacts with growth light and growth rate to alter photosystem II photoinactivation of the coastal diatom *Thalassiosira pseudonana*. *PLoS ONE* 8:e55562. doi: 10.1371/journal.pone.0055562

Magyar, M., Sipka, G., Kovács, L., Ughy, B., Zhu, Q., Han, G., et al. (2018). Rate-limiting steps in the dark-to-light transition of Photosystem II - revealed by chlorophyll-a fluorescence induction. *Sci. Rep.* 8:2755. doi: 10.1038/s41598-018-21195-2

Méléder, V., Laviale, M., Jesus, B., Mouget, J. L., Lavaud, J., Kazemipour, F., et al. (2013). *In vivo* estimation of pigment composition and optical absorption cross-section by spectroradiometry in four aquatic photosynthetic micro-organisms. *J. Photochem. Photobiol. B* 129, 115–124. doi: 10.1016/j.jphotobiol.2013.10.005

Miloslavina, Y., Grouneva, I., Lambrev, P., Lepetit, B., Goss, R., Wilhelm, C., et al. (2009). Ultrafast fluorescence study on the location and mechanism of non-photochemical quenching in diatoms. *Biochim. Biophys. Acta* 1787, 1189–1197. doi: 10.1016/j.bbabio.2009.05.012

Morel, A., Ahn, Y.-H., Partensky, F., Vaulot, D., and Claustre, H. (1993). *Prochlorococcus* and *Synechococcus*: a comparative study of their optical properties in relation to their size and pigmentation. *J. Mar. Res.* 51, 617–649. doi: 10.1357/0022240933223963

Murphy, C. D., Ni, G., Suggett, D. J., Li, G., Barnett, A., Kui, X., et al. (2016). Quantitating active Photosystem II reaction center content from fluorescence induction transients. *Limnol. Oceanogr.* 15, 54–69. doi: 10.1002/lom3.10142

Murphy, C. D., Roodvoets, M. S., Austen, E. J., Dolan, A., Barnett, A., and Campbell, D. A. (2017). Photoinactivation of Photosystem II in *Prochlorococcus* and *Synechococcus*. *PLOS ONE* 12:e0168991. doi: 10.1371/journal.pone.0168991

Ni, G., Zimbalatti, G., Murphy, C. D., Barnett, A. B., Arsenault, C. M., Li, G., et al. (2017). Arctic *Micromonas* uses protein pools and non-photochemical quenching to cope with temperature restrictions on Photosystem II protein turnover. *Photosynth. Res.* 131, 203–220. doi: 10.1007/s11120-016-0310-6

Oliver, R. L., Whittington, J., Lorenz, Z., and Webster, I. T. (2003). The influence of vertical mixing on the photoinhibition of variable chlorophyll a fluorescence and its inclusion in a model of phytoplankton photosynthesis. *J. Plankton Res.* 25, 1107–1129. doi: 10.1093/plankt/25.9.1107

Owens, T. G. (1986). Light-harvesting function in the diatom *Phaeodactylum tricornutum*: II. distribution of excitation energy between the photosystems. *Plant Physiol.* 80, 739–746.

Oxborough, K., and Baker, N. R. (1997). Resolving chlorophyll *a* fluorescence images of photosynthetic efficiency into photochemical and non-photochemical components – calculation of qP and Fv′/Fm′; without measuring Fo′. *Photosynth. Res.* 54, 135–142. doi: 10.1023/A:1005936823310

Oxborough, K., Moore, C. M., Suggett, D. J., Lawson, T., Chan, H. G., and Geider, R. J. (2012). Direct estimation of functional PSII reaction center concentration and PSII electron flux on a volume basis: a new approach to the analysis of Fast Repetition Rate fluorometry (FRRf) data. *Limnol. Oceanogr. Methods* 10, 142–154. doi: 10.4319/lom.2012.10.142

Perkins, R., Williamson, C., Lavaud, J., Mouget, J.-L., and Campbell, D. A. (2018). Time-dependent upregulation of electron transport with concomitant induction of regulated excitation dissipation in Haslea diatoms. *Photosynth. Res.* doi: 10.1007/s11120-018-0508-x. [Epub ahead of print].

R Core Team (2011). *R: A Language and Environment for Statistical Computing*. Vienna: R Foundation for Statistical Computing. Available online at: https://www.R-project.org/

Rast, A., Heinz, S., and Nickelsen, J. (2015). Biogenesis of thylakoid membranes. *Biochim. Biophys. Acta* 1847, 821–830. doi: 10.1016/j.bbabio.2015.01.007

Rocap, G., Larimer, F. W., Lamerdin, J., Malfatti, S., Chain, P., Ahlgren, N. A., et al. (2003). Genome divergence in two *Prochlorococcus* ecotypes reflects oceanic niche differentiation. *Nature* 424, 1042–1047. doi: 10.1038/nature01947

RStudio Team (2015). *RStudio: Integrated Development for R. RStudio, Inc.*, Boston, MA. Available online at: http://www.rstudio.com/

Ruban, A., Lavaud, J., Rousseau, B., Guglielmi, G., Horton, P., and Etienne, A.-L. (2004). The super-excess energy dissipation in diatom algae: comparative analysis with higher plants. *Photosynth. Res.* 82:165. doi: 10.1007/s11120-004-1456-1

Schuback, N., Flecken, M., Maldonado, M. T., and Tortell, P. D. (2016). Diurnal variation in the coupling of photosynthetic electron transport and carbon fixation in iron-limited phytoplankton in the NE subarctic Pacific. *Biogeosciences* 13, 1019–1035. doi: 10.5194/bg-13-1019-2016

Schuback, N., Schallenberg, C., Duckham, C., Maldonado, M. T., and Tortell, P. D. (2015). Interacting effects of light and iron availability on the coupling of photosynthetic electron transport and CO2-assimilation in marine phytoplankton. *PLOS ONE* 10:e0133235. doi: 10.1371/journal.pone.0133235

Serôdio, J., Cruz, S., Vieira, S., and Brotas, V. (2005). Non-photochemical quenching of chlorophyll fluorescence and operation of the xanthophyll cycle in estuarine microphytobenthos. *J. Exp. Mar. Biol. Ecol.* 326, 157–169. doi: 10.1016/j.jembe.2005.05.011

Silsbe, G. M., Oxborough, K., Suggett, D. J., Forster, R. M., Ihnken, S., Komárek, O., et al. (2015). Toward autonomous measurements of photosynthetic electron transport rates: an evaluation of active fluorescence-based measurements of photochemistry. *Limnol. Oceanogr. Methods* 13, 138–155. doi: 10.1002/lom3.10014

Simis, S. G. H., Huot, Y., Babin, M., Seppälä, J., and Metsamaa, L. (2012). Optimization of variable fluorescence measurements of phytoplankton communities with cyanobacteria. *Photosynth. Res.* 112, 13–30. doi: 10.1007/s11120-012-9729-6

Six, C., Finkel, Z., Rodriguez, F., Marie, D., Partensky, F., and Campbell, D. (2008). Contrasting photoacclimation costs in ecotypes of the marine eukaryotic picoplankter *Ostreococcus*. *Limnol. Oceanogr.* 53, 255–265. doi: 10.4319/lo.2008.53.1.0255

Six, C., Finkel, Z. V., Irwin, A. J., and Campbell, D. A. (2007a). Light variability illuminates niche-partitioning among marine picocyanobacteria. *PLoS ONE* 2:e1341. doi: 10.1371/journal.pone.0001341

Six, C., Sherrard, R., Lionard, M., Roy, S., and Campbell, D. (2009). Photosystem II and pigment dynamics among ecotypes of the green alga *Ostreococcus*. *Plant Physiol.* 151, 379–390. doi: 10.1104/pp.109.140566

Six, C., Thomas, J.-C., Garczarek, L., Ostrowski, M., Dufresne, A., Blot, N., et al. (2007b). Diversity and evolution of phycobilisomes in marine *Synechococcus* spp.: a comparative genomics study. *Genome Biol.* 8:R259. doi: 10.1186/gb-2007-8-12-r259

Stirbet, A. (2013). Excitonic connectivity between photosystem II units: what is it, and how to measure it? *Photosynth. Res.* 116, 189–214. doi: 10.1007/s11120-013-9863-9

Suggett, D. J., Goyen, S., Evenhuis, C., Szabó, M., Pettay, D. T., Warner, M. E., et al. (2015). Functional diversity of photobiological traits within the genus Symbiodinium appears to be governed by the interaction of cell size with cladal designation. *New Phytol.* 208, 370–381. doi: 10.1111/nph.13483

Suggett, D. J., Oxborough, K., Baker, N. R., MacIntyre, H. L., Kana, T. M., and Geider, R. J. (2003). Fast repetition rate and pulse amplitude modulation chlorophyll *a* fluorescence measurements for assessment of photosynthetic electron transport in marine phytoplankton. *Eur. J. Phycol.* 38, 371–384. doi: 10.1080/0967026031000161265 5

Suggett, D., MacIntyre, H., and Geider, R. (2004). Evaluation of biophysical and optical determinations of light absorption by photosystem II in phytoplankton. *Limnol. Oceanogr. Methods* 2, 316–332. doi: 10.4319/lom.2004.2.316

Suggett, D., MacIntyre, H., Kana, T., and Geider, R. (2009). Comparing electron transport with gas exchange: parameterising exchange rates between alternative photosynthetic currencies for eukaryotic phytoplankton. *Aquat. Microb. Ecol.* 56, 147–162. doi: 10.3354/ame01303

Swingley, W. D., Iwai, M., Chen, Y., Ozawa, S., Takizawa, K., Takahashi, Y., et al. (2010). Characterization of photosystem I antenna proteins in the prasinophyte *Ostreococcus tauri*. *Biochim. Biophys. Acta* 1797, 1458–1464. doi: 10.1016/j.bbabio.2010.04.017

Trissl, H. W., and Lavergne, J. (1995). Fluorescence induction from Photosystem II: analytical equations for the yields of photochemistry and fluorescence derived from analysis of a model including exciton-radical pair equilibrium and restricted energy transfer between photosynthetic units. *Funct. Plant Biol.* 22, 183–193. doi: 10.1071/pp9950183

Umena, Y., Kawakami, K., Shen, J.-R., and Kamiya, N. (2011). Crystal structure of oxygen-evolving photosystem II at a resolution of 1.9 Å. *Nature* 473, 55–60. doi: 10.1038/nature09913

van Kooten, O., and Snel, J. F. (1990). The use of chlorophyll fluorescence nomenclature in plant stress physiology. *Photosynth. Res.* 25, 147–150. doi: 10.1007/BF00033156

Venables, W. N., and Ripley, B. D. (2002). *Modern Applied Statistics with S-PLUS*. New York, NY: Springer.

Verhoeven, A. (2014). Sustained energy dissipation in winter evergreens. *New Phytol.* 201, 57–65. doi: 10.1111/nph.12466

Ware, M. A., Belgio, E., and Ruban, A. V. (2015). Photoprotective capacity of non-photochemical quenching in plants acclimated to different light intensities. *Photosynth. Res.* 126, 261–274. doi: 10.1007/s11120-015-0102-4

Wilson, A., Boulay, C., Wilde, A., Kerfeld, C., and Kirilovsky, D. (2007). Light-induced energy dissipation in iron-starved *Cyanobacteria*: roles of OCP and IsiA proteins. *Plant Cell* 19, 656–672. doi: 10.1105/tpc.106.045351

Wilson, A., Punginelli, C., Gall, A., Bonetti, C., Alexandre, M., Routaboul, J.-M., et al. (2008). A photoactive carotenoid protein acting as light intensity sensor. *Proc. Natl. Acad. Sci. U.S.A.* 105, 12075–12080. doi: 10.1073/pnas.0804636105

Wu, H., Roy, S., Alami, M., Green, B. R., and Campbell, D. A. (2012). Photosystem II photoinactivation, repair, and protection in marine centric diatoms. *Plant Physiol.* 160, 464–476. doi: 10.1104/pp.112.203067

Xu, K., Grant-Burt, J. L., Donaher, N., and Campbell, D. A. (2017). Connectivity among Photosystem II centers in phytoplankters: patterns and responses. *Biochim. Biophys. Acta* 858, 459–474. doi: 10.1016/j.bbabio.2017.03.003

Zakar, T., Laczko-Dobos, H., Toth, T. N., and Gombos, Z. (2016). Carotenoids assist in cyanobacterial Photosystem II assembly and function. *Front. Plant Sci.* 7:295. doi: 10.3389/fpls.2016.00295

Conflict of Interest Statement: The authors declare that the research was conducted in the absence of any commercial or financial relationships that could be construed as a potential conflict of interest.